ELSEVIER

Journal of Organometallic Chemistry 553 (1998) 307–315

Journal of Organometallic Chemistry

Fixation of triruthenium clusters on melamine: synthesis and structure of $[Ru_3(\mu_2\text{-}H)(CO)_9\{\mu_3,\eta^2\text{-}NHC_3N_3(NH_2)_2\}]$, *cis*-$[\{Ru_3(\mu_2\text{-}H)(CO)_9\}_2\{\mu_3,\eta^2:\mu_3,\eta^2\text{-}NHC_3N_3(NH_2)\}]$ and *trans*-$[\{Ru_3(\mu_2\text{-}H)(CO)_9\}_2\{\mu_3,\eta^2:\mu_3,\eta^2\text{-}NHC_3N_3(NH_2)\}]$

Reto Dorta, Helen Stoeckli-Evans [*], Ulf Bodensieck, Georg Süss-Fink

Institut de Chimie, Université de Neuchâtel, Avenue de Bellevaux 51, Neuchatel CH-2000, Switzerland

Received 9 July 1997; received in revised form 27 August 1997

Abstract

Melamine, $C_3N_3(NH_2)_3$, was found to react with $[Ru_3(CO)_{12}]$ to give, with N–H activation, the monometallated derivative $[Ru_3(\mu_2\text{-}H)(CO)_9\{\mu_3,\eta^2\text{-}NHC_3N_3(NH_2)_2\}]$ (**1**) and the two isomeric bimetallated derivatives *cis*-$[\{Ru_3(\mu\text{-}H)(CO)_9\}_2\{\{\mu_3,\eta^2:\mu_3,\eta^2\text{-}NHC_3N_3(NH_2)\}]$ (*cis*-**2**) and *trans*-$[\{Ru_3(\mu\text{-}H)(CO)_9\}_2\{\mu_3,\eta^2:\mu_3,\eta^2\text{-}NHC_3N_3(NH_2)\}]$ (*trans*-**2**). The molecular structures of **1**, *cis*-**2** and *trans*-**2** have been determined by single-crystal X-ray crystallography. © 1998 Elsevier Science S.A.

Keywords: Ruthenium; Cluster; Multi-cluster; Melamine; X-ray structure

1. Introduction

Ligands containing amido and imido functions have been extensively studied in the coordination chemistry of triruthenium clusters [1]. One of the first compounds isolated and characterised was $[Ru_3(\mu_2\text{-}H)(CO)_{10}(\mu_2\text{-}NHPh)]$, (**A**), accessible from the thermal reaction of $[Ru_3(CO)_{12}]$ with aniline [2]. The imido derivatives of aniline, $[Ru_3(\mu_2\text{-}H)(CO)_9(\mu_3\text{-}NPh)]$ and $[Ru_3(CO)_{10}(\mu_3\text{-}CO)(\mu_3\text{-}NPh)]$, are also known and have been isolated from the reaction between $[Ru_3(CO)_{12}]$ with nitrobenzene [3,4]. These and related complexes are thought to be intermediates in the hydrogenation of nitrobenzene to aniline catalysed by $[Ru_3(CO)_{12}]$ [5].

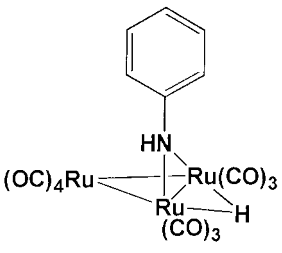

(A)

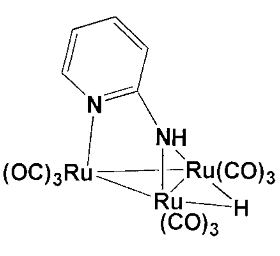

(B)

Ortho-functionalized anilines, such as 1,2-diaminobenzene, have also been studied. With $[Ru_3(CO)_{12}]$, derivatives such as $[Ru_3(\mu_2\text{-}H)(CO)_9\{\mu_2,\eta^2\text{-}NHC_6H_4(NH_2)\}]$ can be obtained [6,7]. The reaction of

---

[*] Corresponding author.

$[Ru_3(CO)_{12}]$ with 2-aminopyridine leads to the formation of $[Ru_3(\mu_2\text{-}H)(CO)_9(\mu_3,\eta^2\text{-}NHC_5H_4N)]$ (**B**) [8,9]. Substituted 2-aminopyridines react in the same way and compounds of the type $[Ru_3(\mu_2\text{-}H)(CO)_9(\mu_3,\eta^2\text{-}NRC_5H_3RN)]$ have been found to have interesting catalytic properties [10,11].

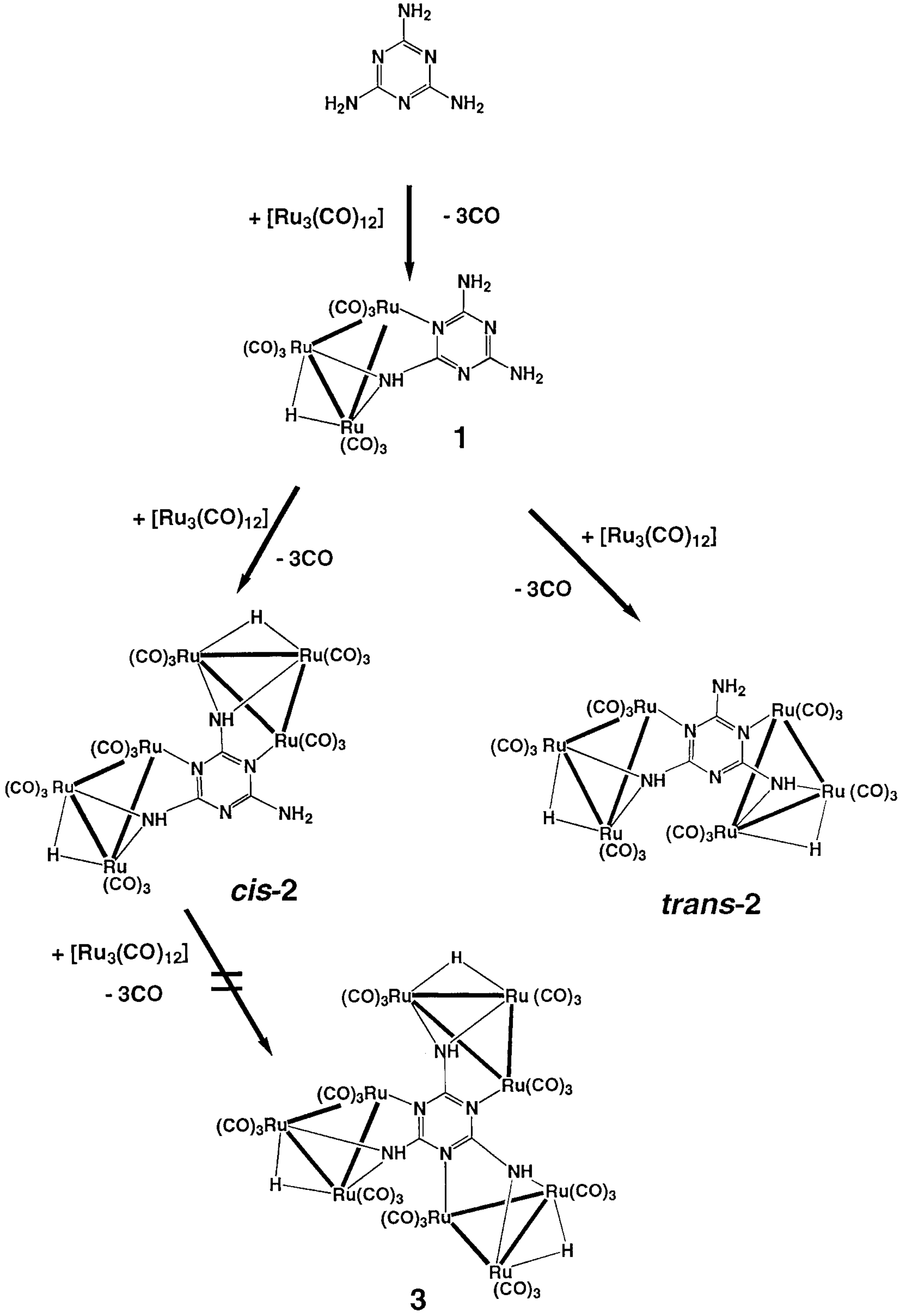

Scheme 1. Thermal reaction of melamine with tri-rutheniumdodecacarbonly.

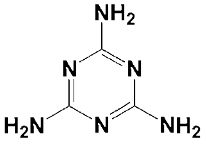

(C)

The chemistry of melamine with first row transition metals has received some attention in recent years [12–15] and monomeric and polymeric complexes of the type ML_2X_n and ML_3X_n, (X being generally halides) have been studied mainly by spectroscopic means. However, to our knowledge, no crystal structure analyses have appeared in the literature. As far as complexes of the type reported here, where more than one metal coordinates to the ligand, the only crystallographic study concerns the similar ligand tri-cyanomelamine. It was shown that polymeric compounds of the type *catena*-[μ_4-tricyanomelamine di-aqua-M^{II}]$\cdot H_2O$, ($M = Co^{II}$, Ni^{II}, Cu^{II} and Cd^{II}) could be formed [16]. In the light of these results, it was decided to initialise a study on the coordination chemistry of melamine, $C_3N_3(NH_2)_3$, (**C**), with trinuclear metal clusters. Here we report on the reaction of melamine with $[Ru_3(CO)_{12}]$.

2. Results and discussion

Melamine offers three possible sites for fixation of the triruthenium cluster. In this way a monometallated, a bimetallated, or a trimetallated derivative could theoretically be formed by activation of one, two or three NH_2 groups of the melamine molecule (Scheme 1). The reaction of $[Ru_3(CO)_{12}]$ at 120°C in THF leads to the formation of a monometallated derivative, **1**, and to two bimetallated isomeric derivatives, *cis*-**2** and *trans*-**2**.

2.1. Synthesis and characterisation of $[Ru_3(\mu_2\text{-}H)(CO)_9\{\mu_3,\eta^2\text{-}NHC_3N_3(NH_2)_2\}]$ (1)

$[Ru_3(CO)_{12}]$ reacts with an equimolar amount of melamine in THF solution at 120°C in a pressure Schlenk tube to give the complex $[Ru_3(\mu_2\text{-}H)(CO)_9\{\mu_3,\eta^2\text{-}NHC_3N_3(NH_2)_2\}]$ (**1**) in good yield (Scheme 1). Complex **1** is an air-stable, orange solid, which was recrystallized from THF. In the infrared spectrum **1** shows the typical $\nu(CO)$ absorption pattern for the $Ru_3(CO)_9$ unit, also observed for $[Ru_3(\mu_2\text{-}H)(CO)_9(\mu_3,\eta^2\text{-}NHC_5H_4N)]$ [8,9]. The ^1H-NMR spectrum of **1** exhibits the signal of a hydride ligand as well as three signals corresponding to the two NH_2 groups and the coordinated NH group (Table 1). The mass spectrum confirmed the molecular composition of **1** by showing the molecular ion peak at $m/e = 682$ (^{101}Ru).

2.2. Synthesis and characterisation of cis-$[\{Ru_3(\mu_2\text{-}H)(CO)_9\}_2\{\mu_3,\eta^2:\mu_3,\eta^2\text{-}NHC_3N_3(NH_2)\}]$(cis-2) and trans-$[\{Ru_3(\mu_2\text{-}H)(CO)_9\}_2\{\mu_3,\eta^2:\mu_3,\eta^2\text{-}NHC_3N_3NH_2)\}]$(trans-2)

With a two fold excess of $[Ru_3(CO)_{12}]$, melamine reacts in THF at 120°C in a pressure Schlenk tube to give a mixture of *cis*-$[\{Ru_3(\mu_2\text{-}H)(CO)_9\}_2\{\mu_3,\eta^2:\mu_3,\eta^2\text{-}NHC_3N_3(NH_2)\}]$ (*cis*-**2**) and *trans*-$[\{Ru_3(\mu_2\text{-}H)(CO)_9\}_2\{\mu_3,\eta^2:\mu_3,\eta^2\text{-}NHC_3N_3(NH_2)\}]$ (*trans*-**2**) together with **1**. Compounds *cis*-**2** and *trans*-**2** can also be synthesized by using **1** as the starting material in the reaction with additional $[Ru_3(CO)_{12}]$ (Scheme 1). Both complexes, *cis*-**2** and *trans*-**2**, show the characteristic $\nu(CO)$ absorption bands of the $Ru_3(CO)_9$ unit in the IR spectrum. The ^1H-NMR spectrum of *cis*-**2**, recorded in $CDCl_3$, shows unexpectedly only one signal at -11.75 ppm for the two non-equivalent hydride ligands; the uncoordinated NH_2 group and the two coordinated NH groups display three signals in the ratio 2:1:1. The proton NMR spectrum of *trans*-**2** was recorded in CD_3COCD_3 (as it was not soluble in $CDCl_3$); it exhibits the signal of the two hydride ligands at -11.59 ppm. In *trans*-**2** the two NH groups cannot be distinguished from each other, giving rise to only one singlet at 6.25 ppm, whereas the signal of the NH_2 group is found at 7.19 ppm. Both *cis*-**2** and *trans*-**2** showed the molecular ion peak at $m/e = 1238$ (^{101}Ru) with the expected Ru_6 isotope pattern in the mass spectrum, the fragmentations of the two isomers being different.

2.3. Structure of $[Ru_3(\mu_2\text{-}H)(CO)_9\{\mu_3,\eta^2\text{-}NHC_3N_3(NH_2)_2\}]$ (1)

The molecular structure of the monometallated complex **1** is illustrated in Fig. 1. The metal framework

Table 1
IR $\nu(CO)$ and ^1H-NMR spectroscopic data for clusters **1**, *cis*-**2** and *trans*-**2**

Complex	$\nu(CO)$ [cm^{-1}]^a	$\delta(^1H)$ [ppm]^b
1	2079(m), 2049(s), 2024(vs), 1991(s), 1955(m)	-11.69 (s, 1H, Ru_2H), 4.20 (s, 1H, NH), 5.08 (s, 2H, NH_2), 5.53 (s, 2H, NH_2)
cis-**2**	2082(vs), 2063(m), 2036(vs), 1994(vs), 1962(m)	-11.75 (s, 2H, Ru_2H), 4.28 (s, 1H, NH), 4.62 (s, 1H, NH), 5.93 (s, 2H, NH_2)
trans-**2**	2082(vs), 2060(m), 2032(vs), 1996(vs), 1948(m)	-11.59 (s, 2H, Ru_2H), 6.25 (s, 2H, NH), 7.19 (s, 2H, NH_2)

^{a}In THF; ^{b}in $CDCl_3$ (**1**, *cis*-**2**) or CD_3COCD_3 (*trans*-**2**).

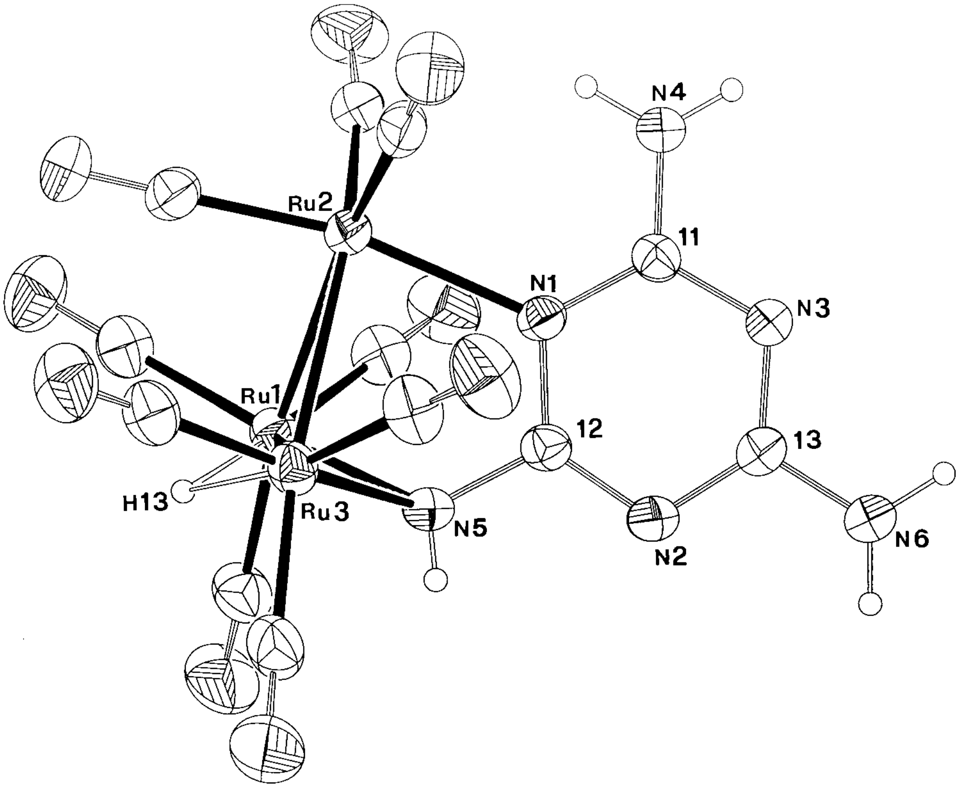

Fig. 1. View of $[Ru_3(\mu_2\text{-H})(CO)_9\{\mu_3,\eta^2\text{-NHC}_3N_3(NH_2)_2\}]$ (**1**) showing the numbering scheme used and thermal ellipsoids at 30% probability.

consists of a nearly equilateral triangle of ruthenium atoms [Ru(1)–Ru(2) 2.750(1), Ru(1)–Ru(3) 2.779(1), Ru(2)–Ru(3) 2.757(1) Å] with each ruthenium atom bonded to three carbonyl groups. The melamine ligand is attached to atom Ru(2) through the aromatic nitrogen N(1) [Ru(2)–N(1) 2.187(4) Å]. The exocyclic nitrogen N(5) bridges the other two ruthenium atoms [Ru(1)–N(5) 2.119(5, Ru(3)–N(5) 2.141(5) Å]. The Ru(1)–Ru(3) edge is bridged by a hydride [H(13)] and is slightly longer than the other two edges (ca. 0.03 Å) (Table 2). On fixation to the triruthenium framework a lengthening of the C–N(amine) bond was observed. Distance C(12)–N(5) is 1.369(6) Å compared to 1.323(7) and 1.329(7) Å for the C–NH_2 bonds, C(11)–N(4) and

Table 2
A comparison of similar bond distances [Å] and angles [°] in complexes **1**, *cis*-**2** and *trans*-**2**

1		*cis*-**2a**		*cis*-**2b**		*trans*-**2**	
Ru1–Ru2	2.750(1)	Ru1–Ru2	2.749(1)	Ru21–Ru22	2.744(1)	Ru1–Ru2	2.748(1)
Ru2–Ru3	2.757(1)	Ru3–Ru4	2.745(2)	Ru23–Ru24	2.753(2)	Ru2–Ru3	2.753(1)
Ru1–Ru3	2.779(1)	Ru1–Ru1[a]	2.776(2)	Ru21–Ru21[a]	2.763(2)	Ru1–Ru3	2.784(1)
		Ru3–Ru3[a]	2.784(2)	Ru23–Ru23[a]	2.774(2)		
Ru2–N1	2.187(4)	Ru2–N1	2.175(11)	Ru22–N21	2.166(12)	Ru2–N1	2.194(5)
		Ru4–N3	2.190(12)	Ru24–N23	2.191(11)		
Ru1–N5	2.119(5)	Ru1–N5	2.151(9)	Ru21–N25	2.163(9)	Ru1–N5	2.146(6)
Ru3–N5	2.141(5)	Ru3–N4	2.171(9)	Ru23–N24	2.139(9)	Ru3–N5	2.147(6)
Ru1–H13	1.81(6)	Ru1–H11	1.75(6)	Ru21–H211	1.83(8)	Ru1–H13	1.83(6)
Ru3–H13	1.77(6)					Ru3–H13	1.70(6)
		Ru3–H33	1.80(8)	Ru23–H233	1.86(11)		
Ru1–H13–Ru3	102(3)	Ru1–H11–Ru1[a]	105(5)	Ru21–H211–Ru21[a]	98(5)	Ru1–H13–Ru3	103(3)
		Ru3–H33–Ru3[a]	101(6)	Ru23–H233–Ru23[a]	97(8)		
C11–N4	1.322(7)		1.38(2)		1.39(2)		1.338(12)
C12–N5	1.369(6)		1.38(2)		1.38(2)		1.366(9)
C13–N6	1.323(7)		1.32(2)		1.30(2)		1.366(9)[b]

[a] Symmetry operation: $x, -y+3/2, z$. [b] C13[a]–N6[a].

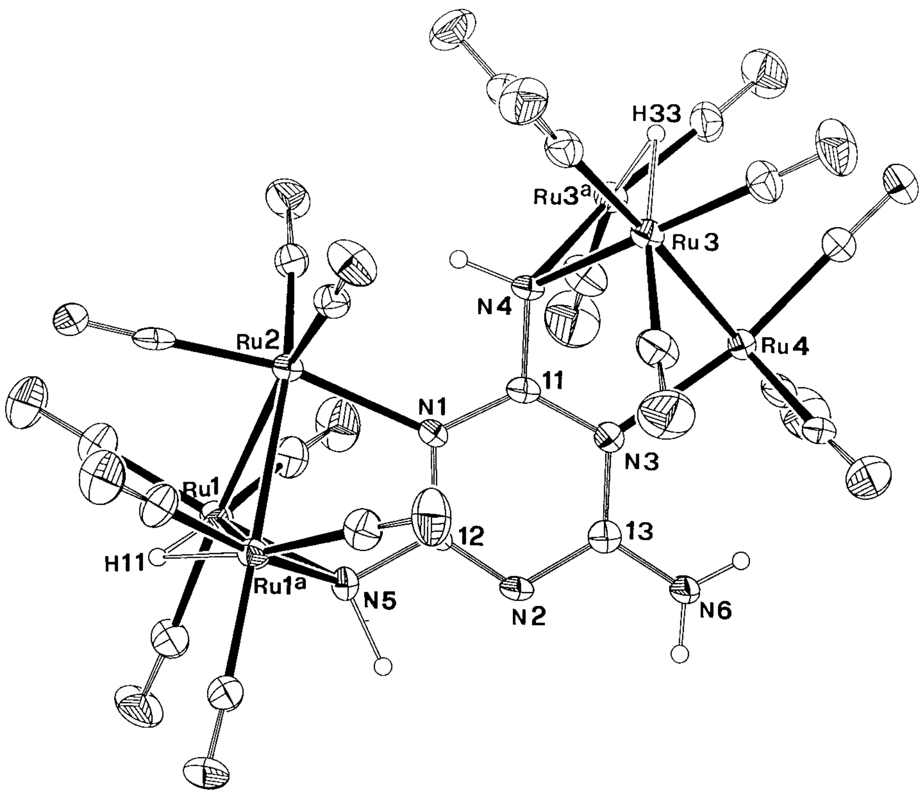

Fig. 2. View of molecule **a** of *cis*-[{$Ru_3(\mu_2\text{-}H)(CO)_9$}$_2${$\mu_3,\eta^2:\mu_3,\eta^2\text{-}NHC_3N_3(NH_2)$}] (*cis*-**2**) showing the numbering scheme used and thermal ellipsoids at 30% probability.

C(13)–N(6), respectively. The structure of **1** can be compared to that of [$Ru_3(\mu_2\text{-}H)(CO)_9$([$\mu_3,\eta^2\text{-}NPhC_5H_4N$)] [8,9]. It shows the same structural properties with very similar bond lengths and angles. It also parallels that of the osmium cluster complex [$Os_3(\mu_2\text{-}H)(\mu_3,\eta^2\text{-}NHC_5H_4N)$] [17].

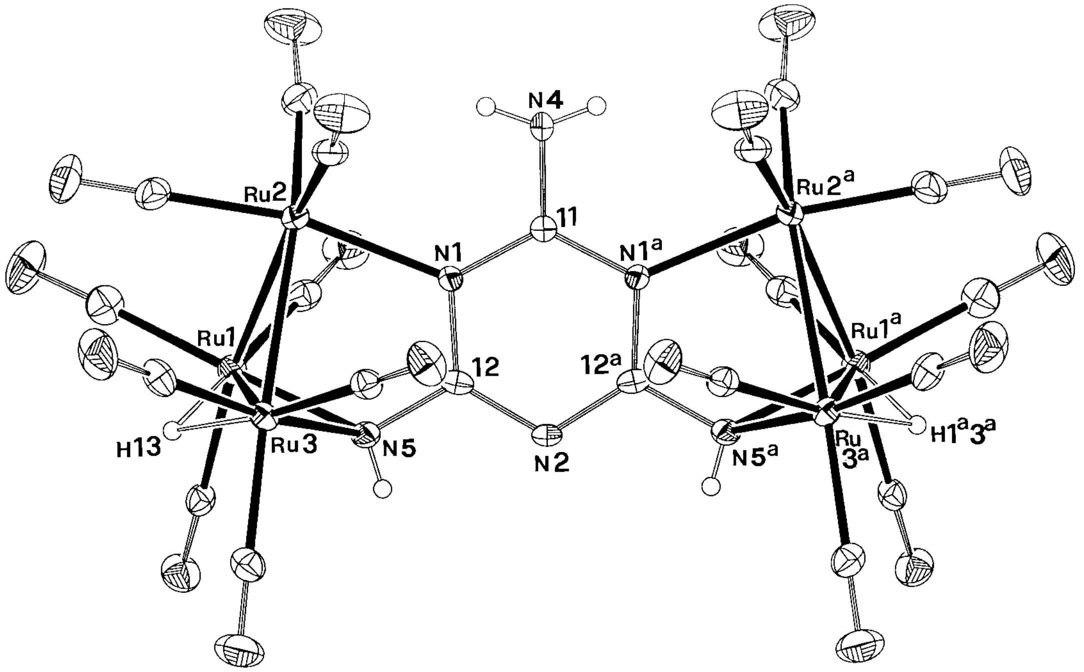

Fig. 3. View of *trans*-[{$Ru_3(\mu_2\text{-}H)(CO)_9$}$_2${$\mu_3,\eta^2:\mu_3,\eta^2\text{-}NHC_3N_3(NH_2)$}] (*trans*-**2**) showing the numbering scheme used and thermal ellipsoids at 30% probability.

*2.4. Structure of cis-[{$Ru_3(\mu_2$-H)$(CO)_9\}_2\{\mu_3,\eta^2:\mu_3,\eta^2$-$NHC_3N_3(NH_2)$}] (cis-**2**)*

The structure of this bimetallated complex, *cis*-**2**, is illustrated in Fig. 2. There are two independent molecules per asymmetric unit (**a** + **b**); both possess Cs symmetry. The melamine moiety lies in the mirror plane which bisects the two Ru_3 triangles. The two $Ru_3(CO)_9$ units are attached *cis* with respect to the ligand, the coordination mode being the same as for **1**. The bond lengths and angles are also similar to those found for complex **1**. In both metal clusters the Ru–Ru edges bridged by the hydrides are slightly longer than the other two Ru–Ru distances (2.78 compared to 2.75 Å in molecule *cis*-**2a**; average values). On comparing the bond lengths between the two metal fragments (Ru(1), Ru(1^a), Ru(2) and Ru(3), Ru(3^a), Ru(4)) and the ligand, it can be seen that the Ru–N(aromatic) bond lengths differ by as much as 0.15 Å in molecule **a**, and by 0.25 Å in molecule **b**. Bond Ru(2)–N(1) (2.175(11) Å) is shorter than the corresponding Ru(4)–N(3) bond length (2.190(12) Å) in molecule *cis*-**2a**; the latter being closer to the value observed in **1** (2.187(4) Å). It can also be seen that the bridging Ru–N(amine) bond lengths are asymmetrical and are longer in *cis*-**2** than those observed in **1**, see Table 2. Again, on fixation of the two Ru_3 skeletons to melamine a lengthening of the C–N(amine) bonds was observed. Distance C(11)–N(4) and C(12)–N(5) were both 1.38(2) Å, in comparison to the C–NH_2 bond, C(13)–N(6), which is 1.32(2) Å. This is similar to the values observed in **1**.

*2.5. Structure of trans-[{$Ru_3(\mu_2$-H)$(CO)_9\}_2\{\mu_3,\eta^2:\mu_3,\eta^2$-$NHC_3N_3(NH_2)$}] (trans-**2**)*

The structure of this second bimetallated complex *trans*-**2** is shown in Fig. 3. The two $Ru_3(CO)_9$ units are now placed *trans* with respect to the melamine ligand and again show a nearly equilateral triangular arrangement. The molecule also possesses C_s symmetry but this time the plane of symmetry bisects the ligand molecule. The triazine ring, however, is still planar, within experimental error. The longest Ru–N(aromatic) bond Ru(2)–N(1) is 2.194(5) Å compared to 2.187 Å in **1** and values ranging from 2.166 to 2.191 Å in *cis*-**2**. The bridging Ru–N(amine) distances Ru(1)–N(5) and Ru(3)–N(5), are symmetrical with a value of 2.147(6) Å. The bridging distance Ru(1)–Ru(3) is 2.784(1) Å, which is similar to the same distance in *cis*-**2a**, but slightly longer than that observed in **1** and *cis*-**2b**, respectively. In *trans*-**2** bond C(12)–N(5)[=C(12^a)–N(5^a)], fixed to the Ru_3 framework is 1.366(9) Å. Again, this is longer than the C–NH_2 bond C(11)–N(4) [1.338(12) Å].

3. Conclusions

Melamine, containing three nitrogen atoms as part of a six-member aromatic heterocycle and three amino substituents at the three carbon atoms of the cycle, represents an extremely interesting ligand system for trinuclear ruthenium cluster chemistry. As expected, the reaction with $[Ru_3(CO)_{12}]$ leads to the formation of the monometallated compound **1** and the two bimetallated isomers *cis*-**2** and *trans*-**2**, by N–H activation of one and two NH_2 groups of the melamine molecule, respectively. The trimetallated derivative [{$Ru_3(\mu_2$-H)$(CO)_9\}_3\{\mu_3,\eta^2:\mu_3,\eta^2:\mu_3,\eta^2$-$NHC_3N_3$}] (**3**) was not detected in the reaction mixture (Scheme 1). It was thought that this compound may be produced from the reaction of *cis*-**2** with additional $[Ru_3(CO)_{12}]$. However, *cis*-**2** did not react with excess $[Ru_3(CO)_{12}]$, even under forcing conditions. The steric requirements for the formation of **3** must be quite severe and the observed rigidity of the triazine ring may explain why this species could not be synthesised here.

4. Experimental section

All reactions were carried out using standard Schlenk techniques under an atmosphere of dried N_2. Thermolysis reactions were performed in high-pressure Schlenk tubes which are able to withstand 8 bar of internal pressure. For preparative thin-layer chromatography, plates were prepared by placing a uniform 0.5 mm layer of Al_2O_3 on 20 × 20 cm glass plates. Solvents were purified and dried prior to use. Melamine was used as received. Infrared spectra were recorded using a Perkin-Elmer 1720 X spectrometer; ^{1}H-NMR spectra were measured using a Varian Gemini 200 BB spectrometer. Elemental analyses were performed by the Mikroelementaranalytisches Laboratorium ETH, Zürich, Switzerland. FAB mass spectra were measured by Prof. T.A. Jenny of the University of Fribourg, Switzerland.

4.1. X-ray crystallography

Data were collected on a Stoe–Siemens AED 2 four-circle diffractometer using graphite-monochromatized Mo Kα radiation ($\lambda = 0.71073$ Å) using $\omega/2\theta$ scans. The structures were solved by direct methods using the program SHELXS-86 [18] and refined by full-matrix least-squares on F^2 using SHELXL-93 [18].

Details of data collection and structure refinement for complexes **1**, *cis*-**2** and *trans*-**2** are given in Table 3. The complexes were all orange in colour and grown from a THF solution at −30°C, 4°C and room temperature, respectively. The three compounds were measured

Table 3
Crystallographic and refinement data for **1**, *cis*-**2**, and *trans*-**2**

Compound	**1**	*cis*-**2**	*trans*-**2**
Empirical formula	$C_{12}H_6N_6O_9Ru_3 \cdot 4\,(C_4H_8O)$	$C_{21}H_6N_6O_{18}Ru_6 \cdot 3\,(C_4H_8O) \cdot 0.5\,H_2O$	$C_{21}H_6N_6O_{18}Ru_6 \cdot C_4H_8O$
Formula weight	969.85	1462.12	1308.87
Temperature (K)	243(2)	223(2)	223(2)
Crystal system	Triclinic	Monoclinic	Orthorhombic
Space group	$P\bar{1}$(No. 2)	$P2_1/m$ (No. 11)	*Pnma* (No. 62)
a, b, c (Å)	10.647(2), 13.474(2), 15.269(2)	14.376(4), 15.546(4), 21.673(6)	11.9387(11), 26.085(3), 12.2843(9)
α, β, γ (°)	70.858(11), 72.074(14), 71.49(2)	90, 93.65(3), 90	90, 90, 90
Volume (Å^3)	1911.0(5)	4834(2)	3825.6(6)
Z	2	4	4
D_{calc} (mg m^{-3})	1.686	2.009	2.273
Absorption coefficient (Mo Kα, mm^{-1})	1.236	1.724	2.167
F(000)	968	2828	2488
Crystal size (mm^3)	$1.00 \times 0.46 \times 0.15$	$0.46 \times 0.38 \times 0.30$	$0.27 \times 0.25 \times 0.15$
θ Range (°)	2.07 to 25.01	2.11 to 25.54	2.38 to 25.49
h, k, l Ranges	−11 to 12, −14 to 16, 0 to 18	−17 to 17, 0 to 18, 0 to 26	0 to 14, −31 to 0, 0 to 14
Reflections collected	7503	9378	3843
Independent reflections	6728 [R(int) = 0.0871]	9371	3646 [R(int) = 0.0624]
Observed reflections [$I > 2\sigma(I)$]	5803	6842	2964
Data/restraints/parameters	6727/0/512	9371/0/618	3646/0/296
Goodness-of-fit on F^2	1.028	1.148	1.149
[a]Final R indices [$I > 2\sigma(I)$]	$R_1 = 0.0466$, $wR_2 = 0.1211$	$R_1 = 0.0712$, $wR_2 = 0.1322$	$R_1 = 0.0441$, $wR_2 = 0.0854$
[a]R indices (all data)	$R_1 = 0.0559$, $wR_2 = 0.1284$	$R_1 = 0.1093$, $wR_2 = 0.1458$	$R_1 = 0.0626$, $wR_2 = 0.0920$
Extinction coefficient	0.0009(4)	0.00000(3)	0.00013(3)
Largest diff. peak and hole (e Å^{-3})	0.847 and −0.602	1.077 and −1.246	0.878 and −0.672
Empirical absorption correction	DIFABS	DIFABS	DIFABS
Transmission factors: min/max	0.297/1.000	0.725/1.000	0.458/1.000

[a] $R_1 = \Sigma \| F_o | - | F_c \| / \Sigma | F_o |$, $wR_2 = \{\Sigma[w(F_o^2 - F_c^2)^2] / \Sigma[w(F_o)^4]\}^{1/2}$, $w^{-1} = [\sigma(F_o^2) + (waP)^2]$, $P = (F_o^2 + 2F_c^2)/3$.

at low temperatures to avoid loss of solvent during data collection. In the crystals of **1** there were found to be four molecules of THF per molecule of complex. For *cis*-**2** there were three molecules of THF and half a molecule of water and finally for *trans*-**2** there was one molecule of THF per molecule of complex. Selected bond distances and angles of the three compounds are compared in Table 2. Figs. 1–3, illustrating the molecular structures of **1**, *cis*-**2** and *trans*-**2**, respectively, were drawn using the program PLATON [19]. Tables of atomic coordinates and complete tables of bond distances and angles of complexes **1**, *cis*-**2** and *trans*-**2** have been deposited with the Cambridge Cristallographic Data Centre, Union Road, Cambridge CB2 1EW, UK.

4.2. Synthesis of $[Ru_3(\mu_2\text{-}H)(CO)_9\{\mu_3,\eta^2\text{-}NHC_3N_3(NH_2)_2\}]$ (1)

A solution of $[Ru_3(CO)_{12}]$ (200 mg, 0.313 mmol) and melamine (40 mg, 0.317 mmol) in 50 ml THF was stirred at 120°C for 55 min. The pressure Schlenk tube was degassed five times during this period to release the CO pressure formed during the reaction. The solvent was removed and the residue redissolved in THF and separated on TLC plates using a 1:3 mixture of THF and toluene as elutant. **1** was isolated as the main orange band (155 mg, 73%) without detectable side products. Orange crystals of **1** were obtained from THF solutions at -30°C. On drying the crystals, lost solvent and an orange powder was formed. Anal. Found: C, 23.40; H, 1.51; N, 11.78. Calc. for $C_{12}H_6N_6O_9Ru_3 \cdot 0.5$ THF ($M = 717.51$): C, 23.44; H, 1.41; N, 11.71%.

4.3. Syntheses of cis-$[\{Ru_3(\mu_2\text{-}H)(CO)_9\}_2\{\mu_3,\eta^2:\mu_3,\eta^2\text{-}NHC_3N_3(NH_2)\}]$(cis-2) and trans-$[\{Ru_3(\mu_2\text{-}H)(CO)_9\}_2\{\mu_3,\eta^2:\mu_3,\eta^2\text{-}NHC_3N_3(NH_2)\}]$ (trans-2)

A mixture of $[Ru_3(CO)_{12}]$ (575 mg, 0.899 mmol) and melamine (60 mg, 0.476 mmol) was stirred in 120 ml of THF at 120°C in a pressure Schlenk tube. CO was released every 10 min during the reaction. After 90 min, the solution was concentrated to ca. 15 cm^3 and the products were separated by TLC using a 1:3 mixture of THF and toluene as the elutant, giving four bands. The first one contained small amounts of $[Ru_3(CO)_{12}]$, followed by three orange bands containing **1** (157 mg, 26%), **2** (91 mg, 16%) and **3** (107 mg, 19%) respectively. Orange crystals of *cis*-**2** were grown at 4°C from a concentrated THF solution and orange crystals of *trans*-**2** were obtained from a THF solution at room temperature. On drying the crystals of both compounds rapidly lost solvent and powders were formed. Analytical data for *cis*-**2**: Anal. Found: C, 22.33; H, 1.04; N, 6.52. Calc. for $C_{21}H_6N_6O_{18}Ru_6 \cdot 0.75$ THF ($M =$ 1290.79): C, 22.33; H, 0.94; N, 6.51%. Analytical data for *trans*-**2**: Anal. Found: C, 21.70; H, 0.35; N, 6.55. Calc. for $C_{21}H_6N_6O_{18}Ru_6 \cdot 0.5$ THF ($M = 1272.76$): C, 21.70; H, 0.78; N, 6.60%.

4.4. Reaction of $[Ru_3(\mu_2\text{-}H)(CO)_9\{\mu_3,\eta^2\text{-}NHC_3N_3(NH_2)_2\}]$ (1) with $[Ru_3(CO)_{12}]$

A mixture of **1** (200 mg, 0.294 mmol) and $[Ru_3(CO)_{12}]$ (332 mg, 0.519 mmol) was stirred in 100 ml THF at 120°C in a pressure Schlenk tube for 40 min. The CO formed was released every ten minutes during the reaction. Work-up as described in Section 4.2 yielded **1** (76 mg, 38%), *cis*-**2** (47 mg, 13%) and *trans*-**2** (62 mg, 17%) together with unreacted $Ru_3(CO)_{12}$.

4.5. Reaction of cis-$[\{Ru_3(\mu_2\text{-}H)(CO)_9\}_2\{\mu_3,\eta^2:\mu_3,\eta^2\text{-}NHC_3N_3(NH_2)\}]$(cis-2) with $[Ru_3(CO)_{12}]$

A mixture of *cis*-**2** (100 mg, 0.081 mmol) and $[Ru_3(CO)_{12}]$ (60 mg, 0.094 mmol) in 30 ml THF was stirred at 160°C for 35 min in a pressure Schlenk tube. It was degassed four times during this period to release the CO pressure formed during the reaction. The solvent was removed, and the dark brown residue redissolved in THF. Separation on TLC plates gave only a band of unreacted $[Ru_3(CO)_{12}]$ and another one containing unreacted **2**. No other compounds could be isolated.

Acknowledgements

We wish to thank the Swiss National Science Foundation for financial support and the Johnson Matthey Technology Centre for a generous loan of ruthenium trichloride hydrate.

References

[1] M.I. Bruce, M.P. Cifuentes, M.G. Humphrey, Polyhedron 10 (1991) 277.

[2] E. Sappa, L. Milone, J. Organomet. Chem. 61 (1973) 383.

[3] S. Bhaduri, K.S. Gopalkrishnan, G.M. Sheldrick, W. Clegg, D. Stalke, J. Chem. Soc., Dalton Trans. (1983) 2339.

[4] S. Bhaduri, K.S. Gopalkrishnan, W. Clegg, P.G. Jones, G.M. Sheldrick, D. Stalke, J. Chem. Soc., Dalton Trans. (1984) 1765.

[5] F. L'Eplattenier, P. Matthys, F. Calderazzo, Inorg. Chem. 9 (1970) 342.

[6] J.A. Cabeza, M.A. Martinez-Garcia, S. Garcia-Granda, J.F. Van der Maelen, V. Riera, J. Organomet. Chem. 514 (1996) 197.

[7] J.A. Cabeza, V. Riera, M.A. Pellinghelli, A. Tiripicchio, J. Organomet. Chem. 376 (1989) C23.

[8] N. Lugan, F. Laurent, G. Lavigne, T.P. Newcomb, E.W. Liimatta, J.-J. Bonnet, J. Am. Chem. Soc. 112 (1990) 8607.

[9] P.L. Andreu, J.A. Cabeza, V. Riera, Y. Jeannin, D. Miguel, J. Chem. Soc., Dalton Trans. (1990) 2201.

[10] A.J. Deeming, in: E.W. Abel, F.G.A. Stone, G. Wilkinson

(Eds.), Comprehensive Organometallic Chemistry II, Vol. 7, p. 733.
[11] J.A. Cabeza, J.M. Fernandez-Colinas, A. Llamazares, Synlett (1996) 579.
[12] C. Gheorghiu, C. Guran, F. Zalaru, R. Martiniuc, Rev. Chim. (Bucharest) 34 (9) (1983) 815.
[13] R.J. Allen, M.J. Pendlowski, D.L. Gerrad, H.J. Bowley, Thermochim. Acta 115 (1987) 21.
[14] L. Finkelstein, Ts.N. Roginskaya, L.A. Simkima, Izv. Vyssh. Uchebn. Zared. Khim. Khim. Tekhnol. 37 (2) (1994) 51.
[15] M. Bircher, C. Guran, I. Jitarun, Rev. Roum. Chim. 39 (10) (1994) 1203.
[16] B.F. Abrahams, S.J. Egan, B.F. Hoskins, R. Robson, J. Chem. Soc., Chem. Commun. (1996) 1099.
[17] A.J. Deeming, R. Peters, M.B. Hursthouse, J.D.J. Backer-Dirks, J. Chem. Soc., Dalton Trans. (1982) 1205.
[18] G.M. Sheldrick, SHELXS-86, SHELXL-93, Programs for Crystal Structure Determination and Refinement, University of Göttingen, Germany, 1986, 1993.
[19] A.L. Spek, PLATON, Acta Crystallogr. A46 (1990) C34.